

Supplementary Information

Achieving highly efficient bipolar near-ultraviolet emitters via regulating energy-levels of the excited states by co-acceptor system

Yuling Sun,^a Daokun Zhong,^a Siqi Liu,^a Ling Yue,^a Zhao Feng,^a Xuming Deng,^a Xi Chen,^a
Xiaolong Yang,^a Guijiang Zhou^{a,*}

^a School of Chemistry, Xi'an Jiaotong University, Xi'an 710049, P. R. China.

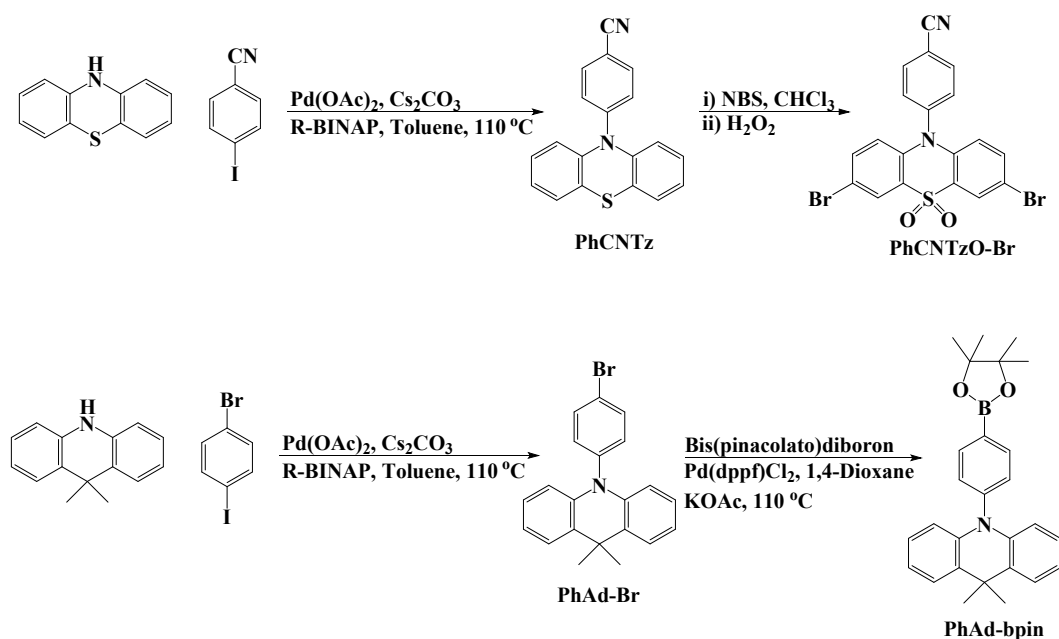
* Corresponding authors

E-mail address: zhougj@mail.xjtu.edu.cn (G. Zhou)

General Information.

Commercial chemicals were used without further purification. All reactions were carried out under nitrogen atmosphere. Prior to use, solvents were carefully dried and distilled from appropriate drying agents. All reactions were monitored by thin-layer chromatography (TLC) from Merck & Co., Inc. Column chromatography and preparative TLC were conducted by using silica gel from Shenghai Qingdao (300–400 mesh). ¹H and ¹³C NMR spectra were recorded in CDCl₃ on a Bruker Avance 400 or 600 MHz spectrometer. Fast atom bombardment mass spectrometry (FAB-MS) spectra were obtained on a Finnigan MAT SSQ710 system. UV-vis spectra were recorded on a Shimadzu UV-2250 spectrophotometer. The photoluminescent spectra and lifetimes of these PhCNTz-based emitters were measured on Edinburgh Instruments FLS920 spectrophotometer. The photoluminescent quantum yields (PLQYs) were determined in toluene solutions, neat film and doped in CzSi film with an integrating sphere. With a scan rate of 100 mV s⁻¹, cyclic voltammetry measurements were carried out on a

Princeton Applied Research model 2273A potentiostat through three-electrode configuration with a glassy carbon working electrode, a Pt-sheet counter electrode and a Pt-wire reference electrode in electrolyte of 0.1 M $[\text{Bu}_4\text{N}]\text{PF}_6$ in degassed *N,N*-Dimethylformamid. All the potentials were quoted with reference to the ferrocene/ferrocenium (Fc/Fc^+) couple as an internal calibrant. The theoretical investigation of geometry optimization was performed with the *Gaussian 09* program package.¹ Density functional theory (DFT) was calculated at Beck's three-parameter hybrid exchange functional² and Lee, and Yang and Parr correlation functional³ B3LYP/6-31G (d). The spin density distributions were visualized using *Gaussview 5.0.8*.



Scheme S1. Synthesis of the Key Intermediate Compounds **PhCNTzO-Br** and **PhAd-bpin**
Synthesis of the key intermediate compounds

General Procedure for Synthesis of PhCNTz and PhAd-Br. Under nitrogen atmosphere, 4-Iodobenzonitrile or 4-bromoiodobenzene. (1.0 equiv), the corresponding donor compound (1.2 equiv), $\text{Pd}(\text{OAc})_2$ (0.03 equiv), (*R*)-(+)-2,2'-bis(diphenylphosphino)-1,1'-binaphthalene (*R*-BINAP, 0.003 equiv) and Cs_2CO_3 (6.0 equiv) were added to a Schlenk tube

containing dry toluene. The resulting mixture was stirred at 110 °C for 18 h. After cooling to room temperature, the mixture was extracted into CH₂Cl₂ and dried with anhydrous Na₂SO₄. After evaporated to dryness, the residue was purified by column chromatography over silica gel using proper eluent.

PhCNTz. CH₂Cl₂: hexene = 1:3 (v/v); Yield: 88%. ¹H NMR (600 MHz, acetone, δ): 7.14-7.19 (m, 2 H), 7.26 (td, *J* = 7.5, 1.5 Hz, 2 H), 7.33 (dd, *J* = 8.1, 1.4 Hz, 2 H), 7.38 (ddd, *J* = 8.5, 7.3, 1.5 Hz, 2 H), 7.49 (dd, *J* = 7.7, 1.4 Hz, 2 H), 7.62-7.66 (m, 2 H).

PhAd-Br. CH₂Cl₂: hexene = 1:3(v/v); Yield: 90%. ¹H NMR (400 MHz, CDCl₃, δ): 7.74 (d, *J* = 8.8 Hz, 2H), 7.44 (d, *J* = 7.6 Hz, 2H), 7.21 (d, *J* = 8.4 Hz, 2H), 6.96 (m, 4H); 6.24 (d, *J* = 8.0 Hz, 2H); 1.68 ppm (s, 6H)

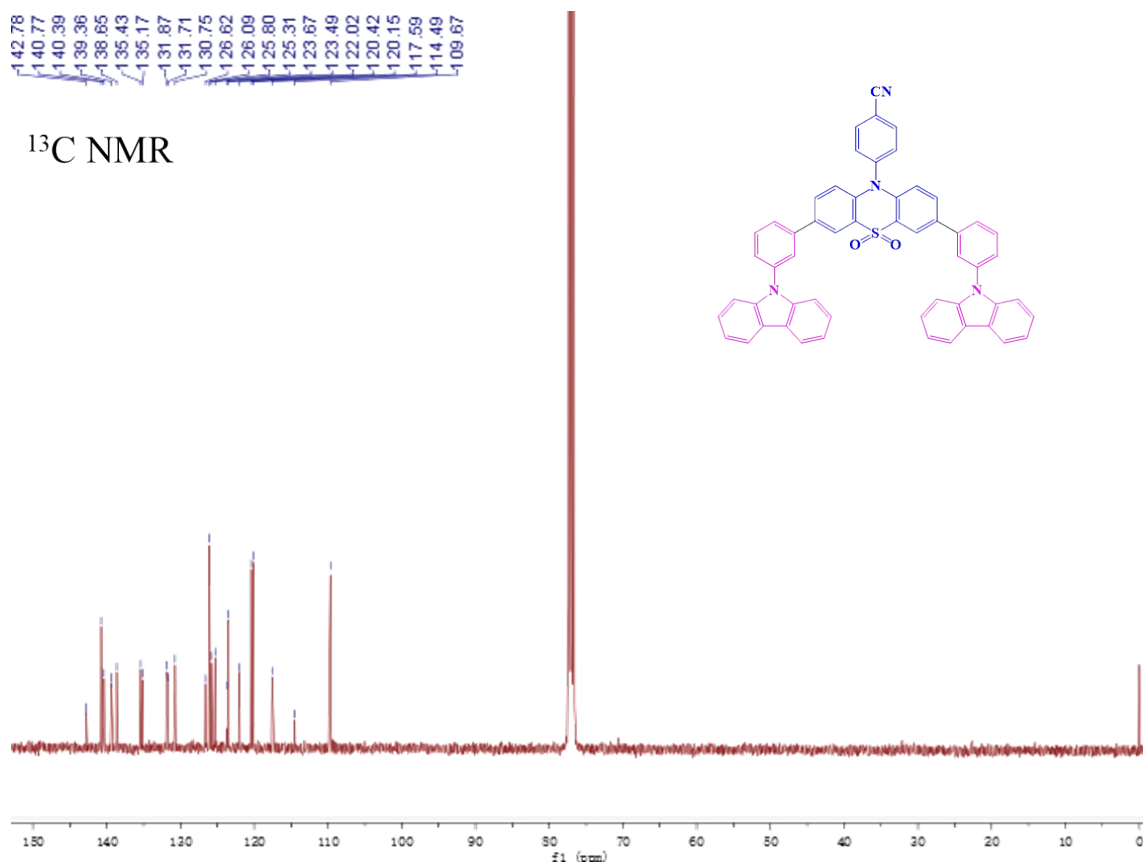
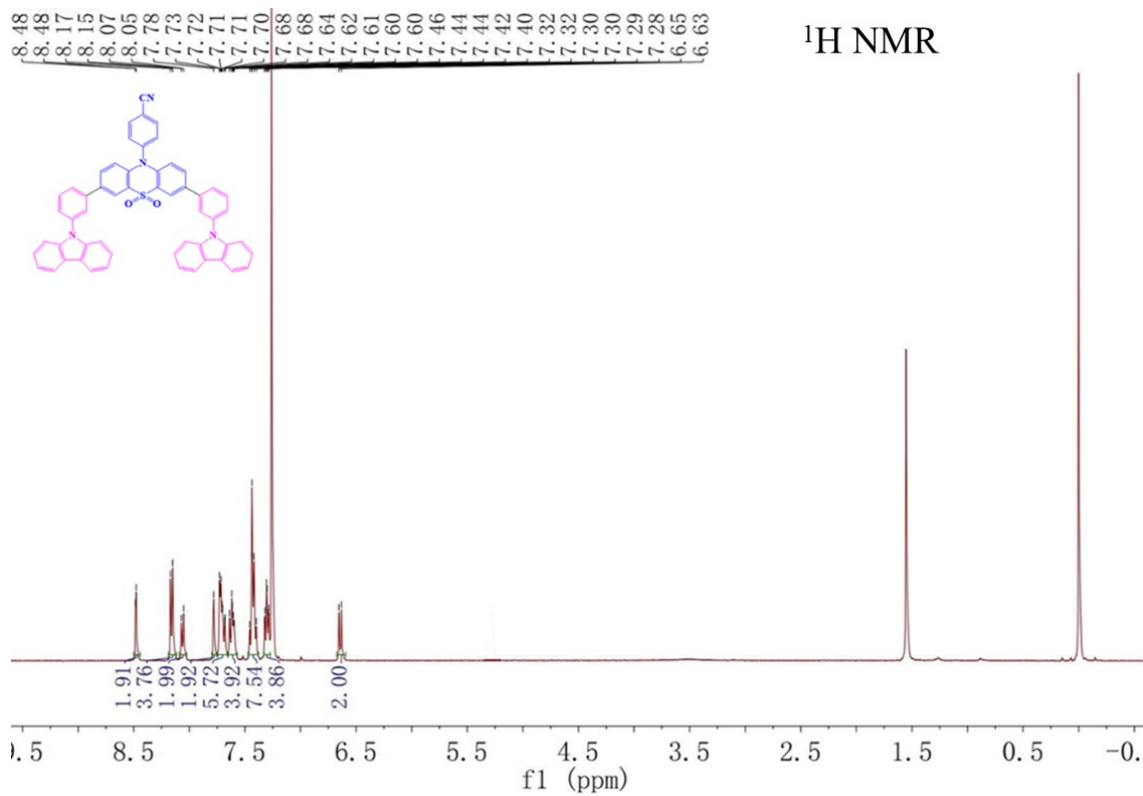
Synthesis of PhCNTzO-Br. Add **PhCNTz** (0.50 g, 1.66 mmol) in to 100 mL round-bottom flask with 20 mL chloroform. And the mixture was placed in an ice bath. After the mixture cooling to 0 °C, N-Bromosuccinimide (0.65 g, 3.66 mmol) was add in three times. The resulting mixture was stirred at room temperature for 4 h. The reaction was detected by TLC, and when **PhCNTz** was completely reacted, excessive hydrogen peroxide was dripped into the mixture. Keep stirring for half an hour, then the mixture was extracted into CH₂Cl₂ and dried with anhydrous Na₂SO₄. After evaporated to dryness, the residue was purified by ethanol recrystallization, got white crystals (0.64 g, 84%). ¹H NMR (400 MHz, CDCl₃, δ): 8.24 (d, *J* = 2.4 Hz, 2H), 8.04 (d, *J* = 8.4 Hz, 2H), 7.55 (d, *J* = 8.5 Hz, 2H), 7.50 (dd, *J* = 9.1, 2.3 Hz, 2H), 6.43 (d, *J* = 9.1 Hz, 2H).

Synthesis of PhAd-bpin. Under nitrogen atmosphere, **PhAd-Br** (0.50 g, 1.37 mmol), Bis(pinacolato)diboron (0.42 g, 1.65 mmol), Pd(dppf)Cl₂ (0.003g, 0.04 mmol) and KOAc (0.54

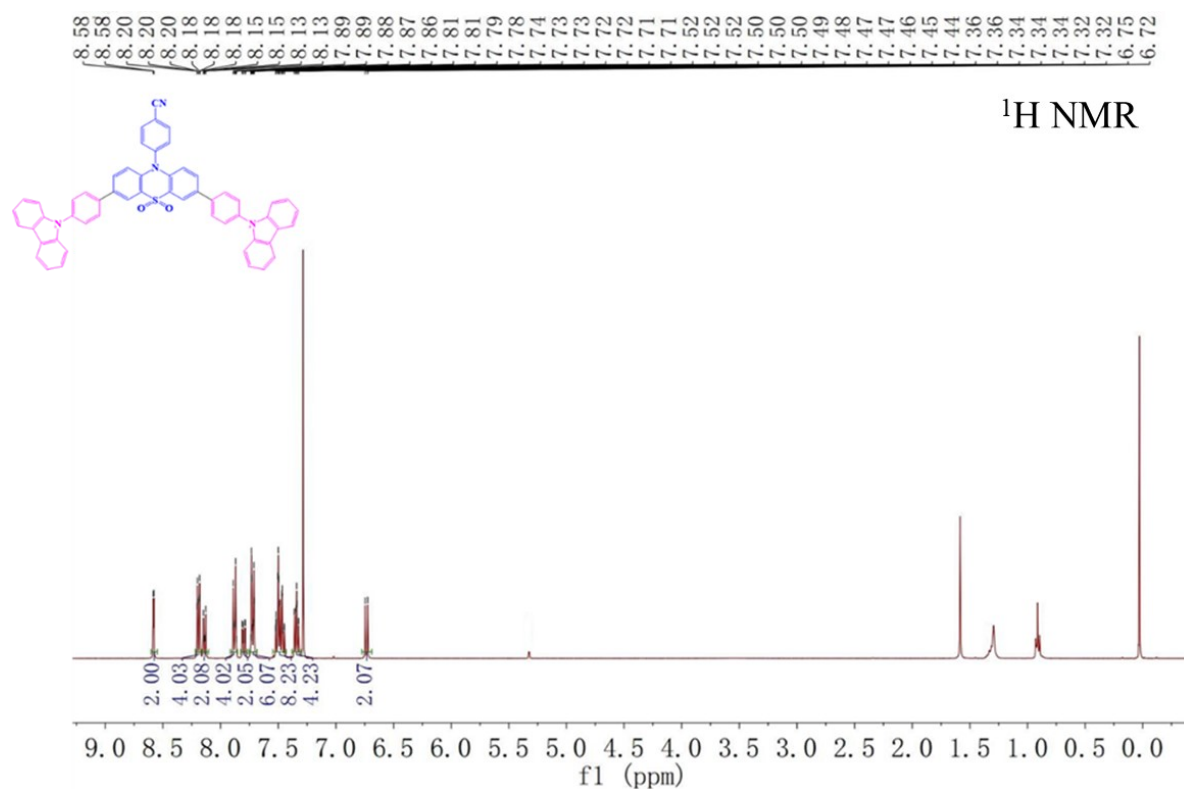
g, 5.49 mmol) were added to a Schlenk tube with degassed 1,4-Dioxane 15 mL. The resulting mixture was stirred at 110 °C for 24 h. After cooling to room temperature, the mixture was filtered, the organic phase was purified by column chromatography over silica gel using hexene flushed, using CH₂Cl₂/hexene (2:1, v/v) as eluent flushed the product, got white solid (0.43 g, 77%). ¹H NMR (400 MHz, CDCl₃, δ): 8.06 (d, *J* = 8.0 Hz, 2H), 7.44 (dd, *J* = 7.5, 1.5 Hz, 2H), 7.34 (d, *J* = 8.5 Hz, 2H), 6.95–6.90 (m, 4H), 6.25 (dd, *J* = 8.0, 1.5 Hz, 2H), 1.69 (s, 6H), 1.400 (s, 12H).

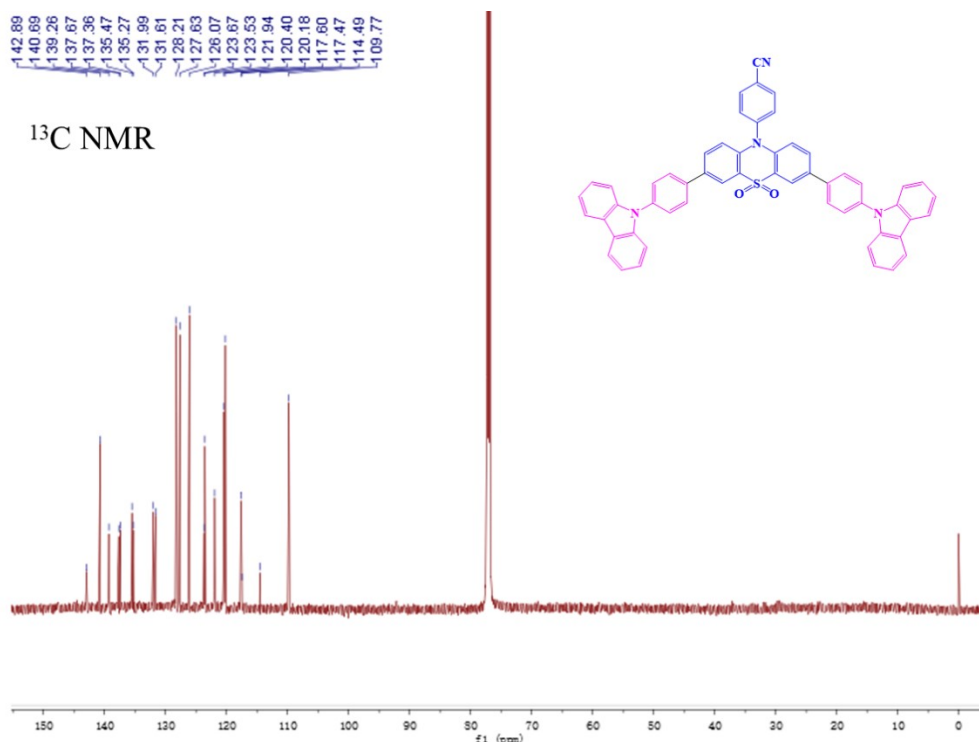
General Procedure for Synthesis of PhCNTzO-*m*Cz, PhCNTzO-Cz and PhCNTzO-Ad. Under nitrogen atmosphere, **PhCNTzO-Br** (1.0 equivalent), (3-(9H-carbazol-9-yl)phenyl)boronic acid, (4-(9H-carbazol-9-yl)phenyl)boronic acid and **PhAd-bpin** (1.3 equivalent) and Pd(PPh₃)₄ (0.03 equivalent) were added to a Schlenk tube containing toluene and K₂CO₃ (aq, 2 M). The resulting mixture was stirred at 110 °C overnight. After cooling to room temperature, the mixture was extracted into CH₂Cl₂ and dried with anhydrous Na₂SO₄. After evaporated to dryness, the residue was purified by column chromatography over silica gel using CH₂Cl₂/ hexene (2:1, v/v) as eluent.

PhCNTzO-*m*Cz: Yield: 90%. ¹H NMR (400 MHz, CDCl₃) δ 8.48 (d, *J* = 2.3 Hz, 2H), 8.16 (d, *J* = 7.7 Hz, 4H), 8.06 (d, *J* = 8.0 Hz, 2H), 7.78 (s, 2H), 7.74 – 7.66 (m, 6H), 7.62 (dd, *J* = 8.1, 5.8 Hz, 4H), 7.50 – 7.36 (m, 8H), 7.30 (td, *J* = 7.1, 6.4, 1.7 Hz, 4H), 6.64 (d, *J* = 8.9 Hz, 2H). ¹³C NMR (101 MHz, CDCl₃) δ 142.78, 140.77, 140.39, 139.36, 138.65, 135.43, 135.17, 131.87, 131.71, 130.75, 126.62, 126.09, 125.80, 125.31, 123.67, 123.49, 122.02, 120.42, 120.16, 117.59, 114.49, 109.67. FAB-MS (*m/z*): 815 [M]⁺; Anal. Calcd for C₅₅H₃₄N₄O₂S: C, 81.06; H, 4.21; N, 6.87; found: C, 81.99; H, 4.23; N, 6.80.

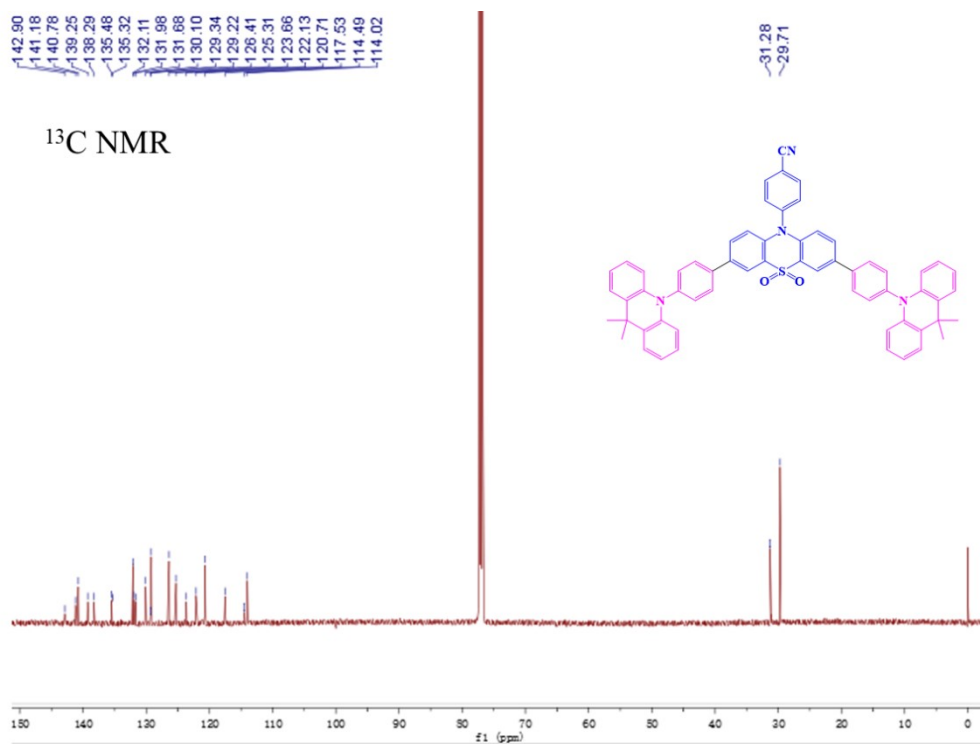
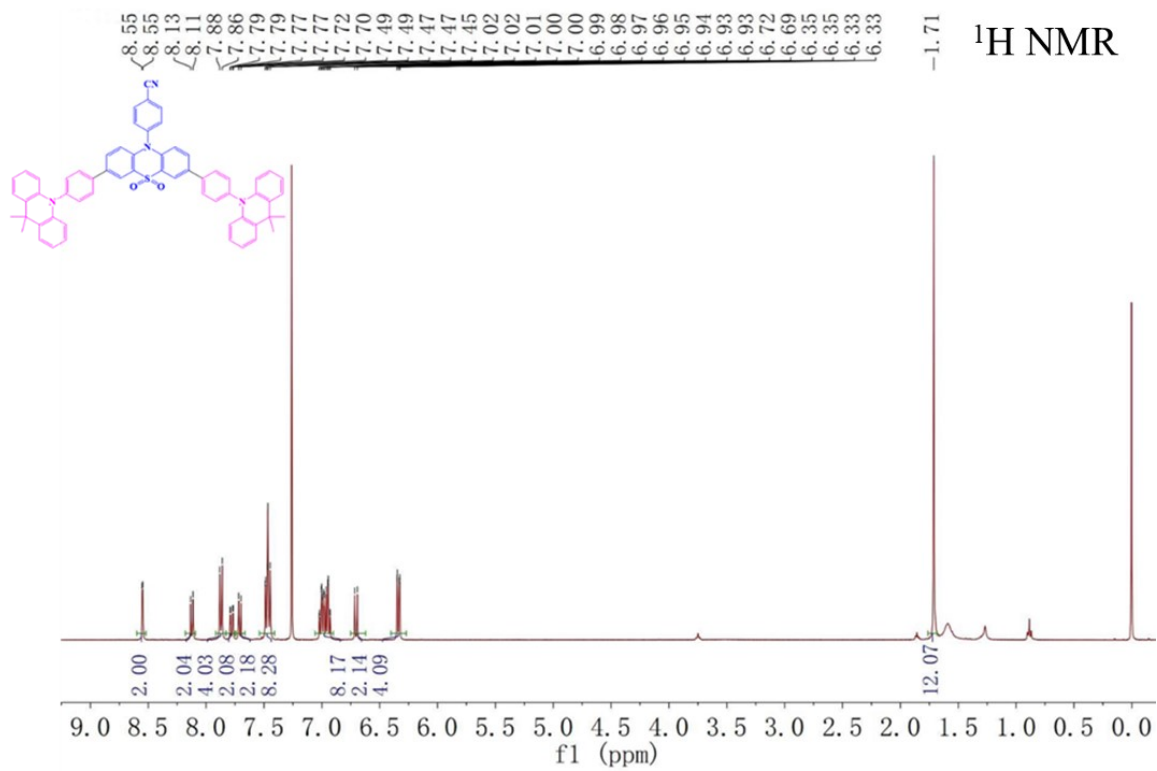


PhCNTzO-Cz: Yield: 89%. ^1H NMR (400 MHz, CDCl_3) δ 8.58 (d, $J = 2.3$ Hz, 2H), 8.19 (d, $J = 7.7$, 1.0 Hz, 4H), 8.14 (d, $J = 8.4$ Hz, 2H), 7.88 (d, $J = 8.5$ Hz, 4H), 7.80 (dd, $J = 8.9$, 2.2 Hz, 2H), 7.77 – 7.65 (m, 6H), 7.56 – 7.39 (m, 8H), 7.34 (td, $J = 8.0$, 6.8, 1.3 Hz, 4H), 6.73 (d, $J = 8.9$ Hz, 2H). ^{13}C NMR (151 MHz, CDCl_3) δ 142.89, 140.69, 139.26, 137.67, 137.36, 135.47, 135.27, 131.99, 131.61, 128.21, 127.63, 126.07, 123.67, 123.53, 121.94, 120.41, 120.18, 117.60, 117.47, 114.49, 109.77. FAB-MS (m/z): 815 $[\text{M}]^+$; Anal. Calcd for $\text{C}_{55}\text{H}_{34}\text{N}_4\text{O}_2\text{S}$: C, 81.06; H, 4.21; N, 6.87; found: C, 81.99; H, 4.23; N, 6.80.





PhCNTzO-Ad Yield: 86%. ¹H NMR (400 MHz, CDCl₃) δ 8.55 (d, *J* = 2.2 Hz, 2H), 8.12 (d, *J* = 8.4 Hz, 2H), 7.87 (d, *J* = 8.4 Hz, 2H), 7.78 (dd, *J* = 8.9, 2.2 Hz, 2H), 7.71 (d, *J* = 8.5 Hz, 2H), 7.63 – 7.38 (m, 8H), 7.16 – 6.87 (m, 8H), 6.70 (d, *J* = 8.9 Hz, 2H), 6.34 (dd, *J* = 8.1, 1.4 Hz, 4H), 1.71 (s, 12H). ¹³C NMR (151 MHz, CDCl₃) δ 142.90, 141.18, 140.78, 139.25, 138.29, 135.48, 135.32, 132.11, 131.98, 131.68, 130.10, 129.34, 129.22, 126.41, 125.31, 123.66, 122.13, 120.71, 117.53, 114.49, 114.02, 31.28, 29.71. FAB-MS (*m/z*): 899 [M]⁺; Anal. Calcd for C₆₁H₄₆N₄O₂S: C, 81.49; H, 5.16; N, 6.23; found: C, 81.39; H, 5.23; N, 6.32.



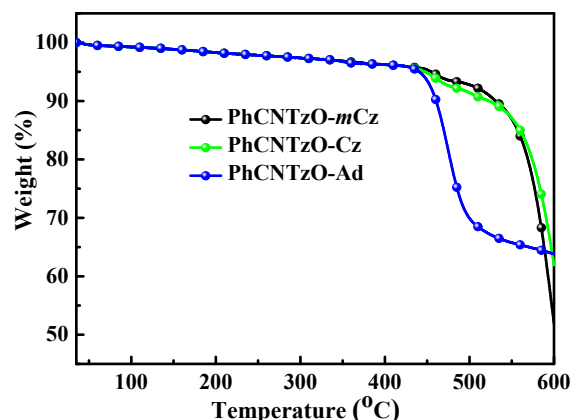


Figure S1. Decomposition temperatures (T_d) curves of PhCNTzO-based NUV emitters

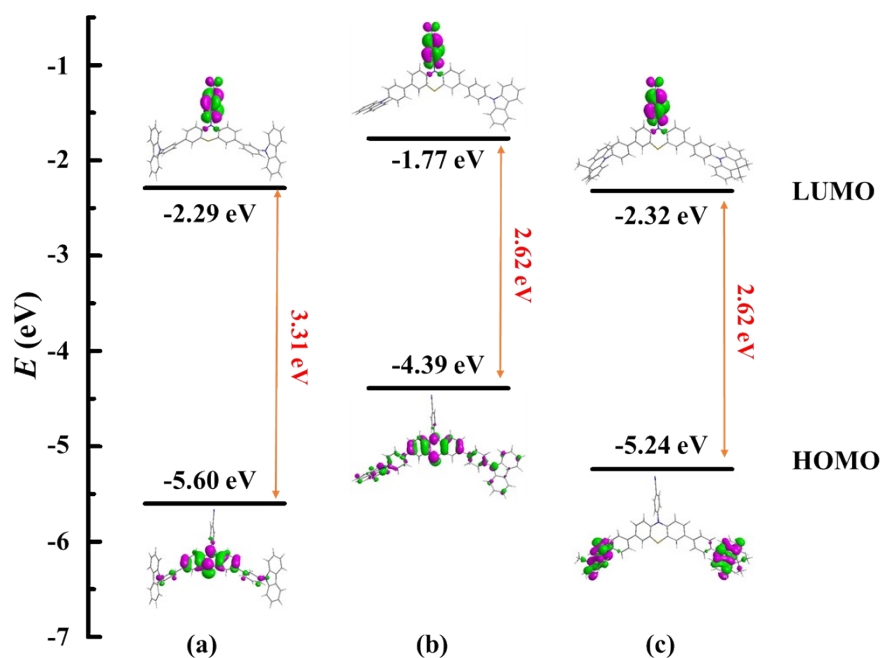


Figure S2. Molecular orbital patterns (isocontour value = 0.025) for the PhCNTz-based emitters based on their optimized S_0 geometries. (a) PhCNTz-*mCz*, (b) PhCNTz-*Cz* and (c) PhCNTz-*Ad*.

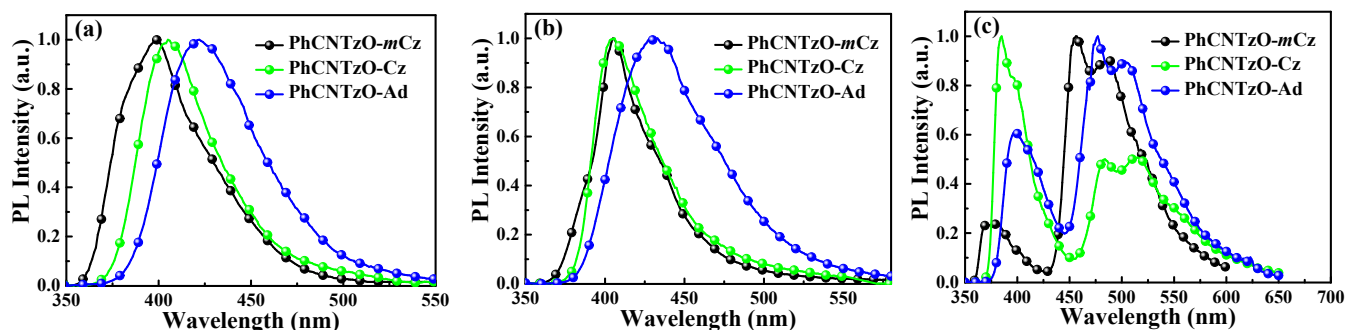


Figure S3. (a) Fluorescence spectra in doped CzSi film (Doping ratio: 10 wt%) and (b) thin film; (c) phosphorescence spectra for these PhCNTzO-based NUV emitters are measured in toluene at 77 K

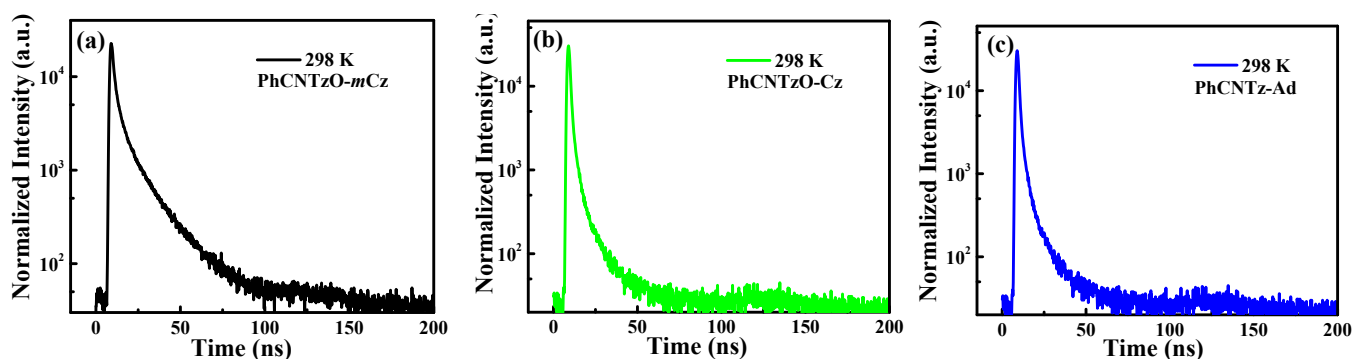


Figure S4. The time decay curves at peak wavelengths of NUV emitters in CzSi film with N_2 atmosphere at 293 K. (a) **PhCNTzO-*m*Cz**, (b) **PhCNTzO-Cz** and (c) **PhCNTzO-Ad**

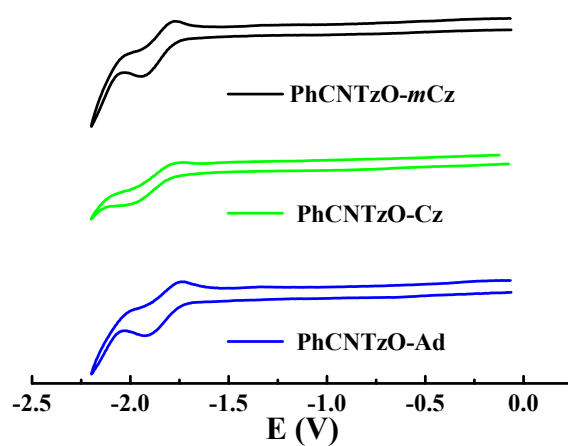
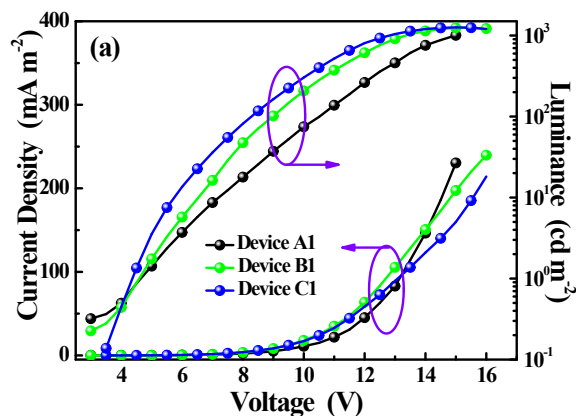


Figure S5. Cyclic curves of these PhCNTzO-based NUV emitters are measured in degassed *N,N*-Dimethylformamide at room temperature.



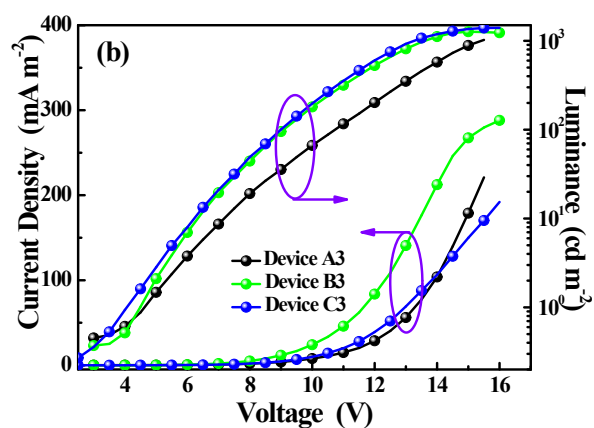


Figure S6. Current density-voltage-luminance (J - V - L) characteristics for the OLEDs based on these PhCNTzO-based emitters.

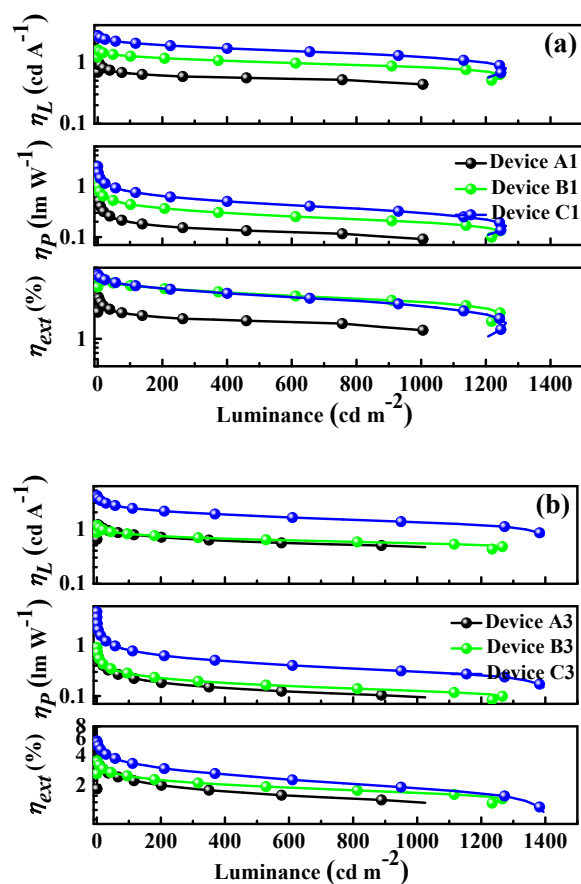


Figure S7 Relationship between EL efficiencies and luminance for the devices based on these PhCNTzO-based emitters.

References

- [1] S. Chen, C.Y. Zhang, H. Xu, Achieving host-free near-ultraviolet electroluminescence via electronic state engineering with phosphine oxide. *Chem. Eng. J.*, 429 (2022), 132327.
- [2] K. O. a. Y. Shirota, New class of hole-blocking amorphous molecular materials and their

application in blue-violet-emitting fluorescent and green-emitting phosphorescent organic electroluminescent devices. *Chem. Mater.*, 15 (2003), 699-707.

[3] Z.-Q. Wang, C.-L. Liu, C.-J. Zheng, W.-Z. Wang, C. Xu, M. Zhu, B.-M. Ji, F. Li and X.-H. Zhang, Efficient violet non-doped organic light-emitting device based on a pyrene derivative with novel molecular structure. *Org. Electron.*, 23 (2015), 179-185.